Remote Sensing of Environment 169 (2015) 163–175

Contents lists available at ScienceDirect

Remote Sensing of Environment

journal homepage: www.elsevier.com/locate/rse

Assimilation of SMOS soil moisture over the Great Lakes basin

Xiaoyong Xu [a,*], Bryan A. Tolson [b], Jonathan Li [a], Ralf M. Staebler [c], Frank Seglenieks [d], Amin Haghnegahdar [b], Bruce Davison [e]

[a] Department of Geography and Environmental Management, University of Waterloo, Waterloo, ON, Canada
[b] Department of Civil and Environmental Engineering, University of Waterloo, Waterloo, ON, Canada
[c] Air Quality Processes Research Section, Environment Canada, Toronto, ON, Canada
[d] Boundary Water Issues, Environment Canada, Burlington, ON, Canada
[e] National Hydrology Research Centre, Environment Canada, Saskatoon, SK, Canada

ARTICLE INFO

Article history:
Received 20 February 2015
Received in revised form 19 May 2015
Accepted 13 August 2015
Available online xxxx

Keywords:
Soil moisture
Assimilation
SMOS
MESH
EnKF

ABSTRACT

The launch of European Space Agency's Soil Moisture and Ocean Salinity (SMOS) satellite has opened up the new opportunities for land data assimilation. In this work, the one-dimensional version of the Ensemble Kalman filter (1D-EnKF) is applied to assimilate SMOS soil moisture retrievals (2010–2013) into a land surface-hydrological model, Modélisation Environmentale-Surface et Hydrologie (MESH), over the Great Lakes basin. A priori rescaling on the retrievals is performed by matching their cumulative distribution function (CDF) to the model surface soil moisture's CDF. The SMOS retrievals, the open-loop soil moisture (no assimilation) and the assimilation estimates are validated against point-scale in situ measurements, respectively, in terms of the daily time series correlation coefficient (skill R). The skill for SMOS retrievals typically decreases with increased canopy density. In contrast, the open-loop model typically provides higher soil moisture skill R for forest surfaces than for crop surfaces. The skill improvement ΔR^{A-M}, defined as the skill for the assimilation soil moisture product minus the skill for the open-loop estimates, for both surface and root-zone soil moisture typically increases as the SMOS observation skill and decreases with increased open-loop skill, showing a strong linear relation to ΔR^{S-M}, defined as the SMOS observation skill minus the open-loop surface soil moisture skill. Every time the SMOS skill is greater than or equal to the open-loop surface soil moisture skill, the assimilation is typically able to significantly improve the model soil moisture skill. The crop-dominated grids typically experience the largest ΔR^{A-M} if the assimilated SMOS retrievals also come from crop surfaces (note that a model grid cell and the SMOS node mapped onto the grid are not exactly matched in space), consistent with a high satellite observation skill and a low open-loop skill, while ΔR^{A-M} is usually weak or even negative for the forest-dominated grids when the SMOS retrievals also from forest surfaces are assimilated, due to the presence of a low observation skill and a high open-loop skill. The dependence of ΔR^{A-S}, referred to as the skill for the surface soil moisture assimilation product minus the SMOS observation skill, upon the open-loop skill and the satellite observation skill is opposite to that for ΔR^{A-M}. Overall our R metric of skill and the anomaly R metric as used in previous studies provide a consistent explanation for the vegetation modulation of the assimilation. This work offers further insight into the impact of the open-loop skill and the satellite observation skill on the assimilation.

1. Introduction

Soil moisture, especially its anomaly information, is critical to weather and climate forecast initialization (e.g., Lau & Kim, 2012; Wolfson, Atlas, & Sud, 1987; Zeng et al., 2014; Zhang & Frederiksen, 2003). Microwave remote sensing technology offers an important approach for soil moisture estimation because changes in soil water content strongly affect the soil's dielectric properties. Satellite microwave remote sensing holds the ability to provide the large-scale spatially distributed near-surface soil moisture estimates, which, relative to point in situ measurements, are more compatible in space with land/hydrologic models, especially the distributed models. In the past decade, satellite microwave soil moisture observations have been intensively integrated into land surface and hydrologic models, in particular through advanced data assimilation that merges the observation and the model forecast based on estimates of their respective error characteristics (see a review paper by Xu, Li, & Tolson, 2014). Data assimilation can spread and smooth the observed information in time and space (Reichle, 2008). Through data assimilation, the remotely-sensed near-surface soil moisture information can be propagated to the soil layers or the model variables that are not directly measured by satellites (e.g. Reichle & Koster, 2005). Additionally, in a data assimilation system

* Corresponding author at: Department of Geography & Environmental Management, University of Waterloo, 200 University Avenue West, Waterloo, Ontario N2L 3G1, Canada.
E-mail address: xiaoyong.xu@uwaterloo.ca (X. Xu).

http://dx.doi.org/10.1016/j.rse.2015.08.017
0034-4257/

satellite retrievals from different platforms can be merged into the same model framework to produce a single optimal state estimation of interest (e.g. Draper, Reichle, De Lannoy, & Liu, 2012).

Until recently, the satellite soil moisture products were mainly based upon the X (8–12 GHz) or C (4–8 GHz) band measurements, such as the Advanced Microwave Scanning Radiometer-Earth Observing System (AMSR-E), the Scanning Multichannel Microwave Radiometer (SMMR), the Tropical Rainfall Measuring Mission Microwave Imager (TMI), the Advanced Scatterometer (ASCAT), and the RADARSAT series. A series of assimilation experiments based upon these products (e.g. Brocca et al., 2010; Crow, Bindlish, & Jackson, 2005; Draper et al., 2012; Drusch, 2007; Liu et al., 2011; Reichle & Koster, 2005; Reichle et al., 2007) have demonstrated the potential of satellite retrievals to improve the predictive capabilities of land surface and hydrologic models (e.g. soil moisture and runoff estimates) and provided insight into the main challenges in this field of research (e.g. the model-satellite scale discrepancy; the statistical biases between satellite product and model estimation). However, X and C band sensors are susceptible to vegetation cover and are sensitive to only the near-surface soil moisture (top 1 to 1.5 cm). The launch of European Space Agency's (ESA) Soil Moisture and Ocean Salinity (SMOS) satellite that carries an L-band (~1.4 GHz) Microwave Imaging Radiometer with Aperture Synthesis (MIRAS) (Kerr et al., 2010, 2001) has opened up the new opportunities for land data assimilation. The assimilation of SMOS soil moisture is more attractive because the L-band microwave has a stronger penetration of vegetation and soil (as opposed to those operating at X or C band), which can provide surface soil moisture estimates for a wide range of vegetation conditions and thus offer the new opportunities for assessing the vegetation modulation of the assimilation.

In recent years, there has been an intensive global research effort to assimilate SMOS soil moisture data in various models (e.g., Ridler, Madsen, Stisen, Bircher, & Fensholt, 2014; Zhao et al., 2014). Zhao et al. (2014) incorporated the SMOS soil moisture retrievals into a land surface model by minimizing the distance of the model solution from the SMOS observation and the background model estimate (by calibrating the model using the SMOS data first), which produced the improved surface soil moisture estimates. However, the study averaged the SMOS data across the entire domain (located in the central Tibetan Plateau) and the assimilation was performed at a coarser scale (~100 km) than the SMOS product scale (~15 km). A more recent study by Ridler et al. (2014) assimilated SMOS soil moisture in a bias-aware system (i.e., the observation bias is estimated jointly with the model state by state augmentation). The assimilation was conducted at a fine scale (by applying a vegetation-based disaggregation scheme to the SMOS observation bias) and led to superior soil moisture estimates (in terms of the square of the correlation), especially for the surface layer, although only one node retrievals were used.

In this paper, an ensemble Kalman filter (EnKF) is applied to assimilate SMOS soil moisture retrievals (Level 2) into a coupled land-surface and hydrological model MESH over the Great Lakes basin. Due to the bias between the retrievals and the model surface soil moisture, a priori rescaling on the SMOS retrievals is performed by matching their cumulative distribution function (CDF) to the model surface soil moisture's CDF. The retrievals, the open-loop model (no assimilation) soil moisture, and the assimilation estimates are validated against in situ soil moisture measurements from the Michigan Automated Weather Network, the Soil Climate Analysis Network, and the Fluxnet-Canada Research Network, in terms of the daily-spaced time series correlation coefficient (soil moisture skill R). Our study differs from previous SMOS assimilation studies in three aspects: (1) the assimilation is conducted at a grid scale similar to the SMOS product scale (~15 km), and the assimilation estimates are validated at both the grid-scale and the subgrid-scale; (2) the Great Lakes basin was chosen as the study domain since it offers a range of vegetation conditions that favor the assessment of the vegetation impact on the assimilation; and (3) 4 years of SMOS data (2010–2013) are used, and the overall consistency between the years strongly demonstrates the robustness of our general conclusions. This paper is organized as follows. In Section 2, the data sets, the forecast model, and the assimilation scheme are described. Section 3 presents the skill for the SMOS soil moisture. Section 4 is focused upon the assimilation results. A summary and discussion is provided in Section 5.

2. Data and methods

2.1. SMOS soil moisture retrievals

In this work, we use the SMOS Level 2 Soil Moisture User Data Product (MIR_SMUDP2) delivered by ESA. The product comprises the instantaneous soil moisture retrievals (rather than the daily composite as provided in the Level 3 product) and abundant reference information, such as geophysical features, retrieved standard deviation (RSTD), etc. The retrieved soil moisture is primarily based upon an iterative algorithm, which matches the modeled L-band emission of the surface to that observed by SMOS/MIRAS (Kerr et al., 2008, 2012). SMOS has a footprint of 43 km on average and a temporal resolution of 1–3 days for both ascending (6:00 am LST) and descending (6:00 pm LST) orbits. The MIR_SMUDP2 soil moisture retrievals are equally spaced at about 15 km (oversampled by a factor of nine). Four years (2010–2013) of SMOS retrievals from both ascending and descending overpasses are used in this study. Utilizing the attached reference information, a filtering is performed to exclude the retrievals with a large RSTD ($>0.08\ m^3/m^3$) and those contaminated by open water, frozen surface, snow, or rain, etc. To conduct the evaluation and assimilation, SMOS retrievals are resampled onto the hydrological forecast model grids (~15 km resolution) using a nearest neighbor approach. Whenever and wherever the model (combined with the rainfall forcing data) indicates the presence of precipitation, frozen soils, or snow cover, the satellite retrievals are also excluded from the evaluation and assimilation. Note that the processor version of the Level 2 product was changed over the four years with V501 (REPR data set) for 2010/2011 and V551 (OPER data set) for 2012/2013. Since different dielectric constant models are used in the two versions, there may be inconsistencies in the absolute magnitude of SMOS retrieval between 2010/2011 and 2012/2013.

2.2. Hydrological model and in situ measurements

The forecast model used here is Environment Canada's standalone MESH (Modélisation Environmentale-Surface et Hydrologie) model (Pietroniro et al., 2007), which originates from the coupling of the land surface scheme CLASS with the hydrological model WATFLOOD (Soulis, Snelgrove, Kouwen, Seglenieks, & Verseghy, 2000). The primary feature of MESH is that the model uses a Grouped Response Unit (GRU) approach to resolve the subgrid-scale variability. A GRU is a grouping of subareas with similar soil and vegetation attributes, and each model grid cell is represented by a limited number of distinct GRUs weighted by their respective cell fractions. In the version of MESH used in this work, the identification of GRUs is based solely on the land cover types, i.e., each GRU corresponds to one land cover class (other soil characteristics are assumed to be same for the same GRU). The soil column is partitioned into three layers (0–10, 10–35, and 35–410 cm) to resolve soil moisture and temperature dynamics. At the moment, the land surface scheme considers only the vertical water movement between the soil layers, which is governed by Richard's equation (Soulis et al., 2000). Within a grid cell, the fluxes and variables are computed independently for GRUs, ignoring the interactions between GRUs. The overall fluxes and prognostic variables of a grid cell are obtained by taking a weighted average of those from GRUs. The lateral movement of water between grid cells is not taken into account. The resulting horizontal flows (overland flow, interflow, and base flow) at grid cells are ultimately be routed into the stream and river network systems.

The study domain for this work is the Great Lakes basin (Fig. 1). The basin, straddling the Canada–United States border, consists of the

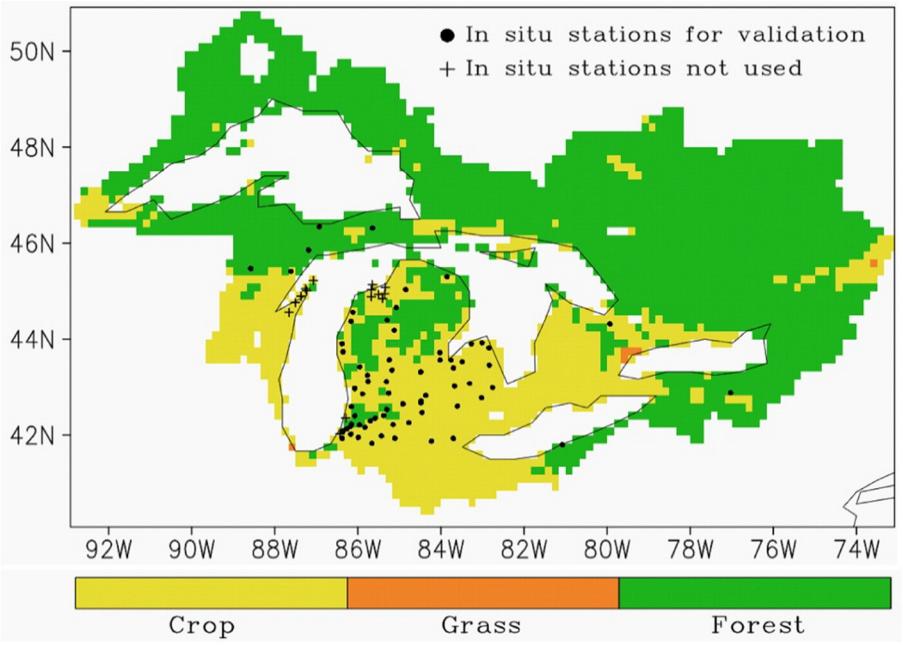

Fig. 1. Vegetation types (gridded at 1/6th of a degree resolution) over the Great Lakes basin and location of in situ stations for soil moisture measurements. In situ stations are from the Michigan Automated Weather Network (79 sites), the Soil Climate Analysis Network (3 sites), and the Fluxnet-Canada Research Network (1 site). Stations that are not used for validation are marked with plus signs (SMOS retrievals are not available or not considered over these stations due to the impact of open water).

largest group of freshwater lakes on earth and the surrounding lands, with a drainage area of about 1,000,000 km^2. The five primary fresh lakes are naturally interconnected and contain roughly one-fifth of the world's fresh surface water supply. The model configurations are similar to those used in Pietroniro et al. (2007) and Haghnegahdar et al. (2014). The model is run at a resolution of 1/6th of a degree (~15 km) using a time step of 30 min. Each model grid cell is divided into a mosaic of GRUs. Each GRU corresponds to one land cover type and is weighted by the fraction of the land cover class within the cell. Seven GRU types are used for this domain, including crop, grass, deciduous forest, coniferous forest, mixed forest, water, and impervious. The land cover types were derived from a United States Geological Survey (USGS) climatological database. In this work, the model parameter sets are directly taken from a global calibration experiment where GRU specific parameters are calibrated basin-wide to streamflow observations (Haghnegahdar et al., 2014). Here MESH is forced using the gridded hourly precipitation data derived from the Canadian Precipitation Analysis (CaPA; Mahfouf, Brasnett, & Gagnon, 2007); other meteorological forcing data (incoming shortwave and longwave radiations, surface air temperature, wind speed, pressure, and specific humidity) come from the Global Environmental Multiscale (GEM) model forecasts (Mailhot et al., 2006).

In this work, in situ soil moisture measurements (Fig. 1) from the Michigan Automated Weather Network (MAWN; http://www.agweather.geo.msu.edu/mawn/), the Soil Climate Analysis Network (SCAN; http://www.wcc.nrcs.usda.gov/scan/), and the Fluxnet-Canada Research Network (FCRN) are used to validate the SMOS retrievals, the model and the assimilation estimates. The specification of in situ stations and measurements is provided as electronic supplement. MAWN is comprised of about 79 stations. Each station uses two Campbell Scientific water content reflectometers (CS615 or CS616) to measure soil moisture. The two probes are horizontally inserted to provide hourly soil moisture measurements at depths of 10 and 25 cm (for 46 MAWN sites) or are vertically installed to measure soil moisture in the upper 60 cm profile (0–30 and 30–60 cm) (for 33 MAWN sites since about the middle of year 2008). Additionally, in situ data from three SCAN sites (SCAN2003, 2011, and 2073) and one FCRN site (the Borden forest station) are included in this study. At SCAN sites, Stevens Hydra Probe sensors are horizontally inserted to provide hourly soil moisture measurements at 5, 10, 20, 50, and 100 cm below the surface, while at the Borden station (44.32°N, 79.93°W) 30 min-averaged soil moisture measurements are taken with CS615 probes at 2, 5, 10, 20, 50, and 100 cm below the surface at two locations. A filtering step is applied to all in situ data to ensure the reliability and effectiveness of the subsequent validations. In situ soil moisture observations are rejected if (1) they are beyond any realistic ranges (e.g., too high or too low to be explained by physical variability); (2) the time series contains sudden changes (significant "jump") that are impossibly attributed to physical process; or (3) the soil is frozen.

2.3. The EnKF method

Data assimilation typically can be viewed as a process to optimally merge the model forecast and the observed information based upon some estimate of their error characteristics. A great number of methods have been developed for land/hydrologic data assimilation (e.g., Crow & Wood, 2003; Crow & Zhan, 2007; Evensen, 1994, 2003; Reichle, Walker, Koster, & Houser, 2002; Reichle et al., 2007). The reader is referred to the relevant articles for details on the properties of different algorithms. In the present study, the ensemble Kalman filter (EnKF) is used to assimilate SMOS soil moisture in the MESH model. The traditional Kalman Filter (KF) and its various variants (extended Kalman Filter, EKF; EnKF) are typical 'filtering' (or sequential) assimilation techniques. In the traditional KF, each assimilation cycle consists of a forecast step and an analysis step. In the forecast step, the forecast model is integrated forward in time (from an initial or analysis state) with an additional error covariance equation (linear model operator) to propagate the error information, while at the analysis step the new observation is used to update the current forecast estimation. The KF is valid only for linear systems. Its nonlinear variant, the EKF, can be utilized to solve the nonlinear optimal estimation problem. The EKF still explicitly estimates and propagates the error information, but with a linearized and approximate error covariance equation. In practice, however, the full error covariances are difficult or impossible to directly estimate due to an expensive computational cost and insufficient error information, especially for large-scale applications. Additionally, the EKF may not be

suitable for highly nonlinear systems since the high-order moments are ignored in its error covariance equation. To this end, Evensen (1994) proposed the EnKF scheme.

The primary innovation of the EnKF is that a Monte Carlo approach is used to estimate model and measurement error statistics. The probability density of the model states is represented using an ensemble where the mean is the best estimate (Gaussian assumption), and the ensemble spread defines the error variance. The model error statistics evolve by integrating the ensemble of model states forward in time. The measurement errors are represented using another ensemble with the mean equal to zero (Gaussian assumption) and the spreading of the ensemble consistent with the realistic or predefined observation error variance. The measurement errors are imposed onto the actual measurement to yield the ensemble of observations. At measurement times, a variance-minimizing analysis is applied to the ensemble of model forecast states, given by

$$x_j^+ = x_j^- + P^- H^T \left[H P^- H^T + R \right]^{-1} \left[y_j - H x_j^- \right], j = 1, \ldots, N \quad (1)$$

where j is the ensemble member index, counting from 1 to the ensemble size N. x_j^- and x_j^+ denote the a priori and posterior model state estimates, respectively. y_j represents the perturbed observation. H is the measurement operator. P^- and R denote the error covariances for model forecast and observation, respectively. In contrast to the EKF, the error evolution is implicit and fully nonlinear in the EnKF but with a lower rank (finite ensemble size).

3. Skill for SMOS soil moisture

SMOS soil moisture products have been evaluated over different regions/scales with in-situ data from point (e.g. Al Bitar et al., 2012; Albergel et al., 2012) or network measurements (e.g. Gherboudj et al., 2012; Jackson et al., 2012; Ridler et al., 2014; Zhao et al., 2014). The validation studies have suggested that the SMOS retrievals typically exhibit an underestimation bias. The performance of the retrievals varies with the scale of the validation, typically showing a better accuracy for a large-scale average. Overall the desired accuracy of 0.04 m^3/m^3 for SMOS retrievals is met wherever the vegetation cover is light (nominal surfaces). However, the validation of coarse-scale satellite soil moisture unavoidably suffers from the disparity in spatial representativeness between satellite products and ground measurements (Crow et al., 2012; Jackson et al., 2010). Point-scale ground measurements, relative to the spatial averages, typically contain large uncertainties, which are strongly controlled by the precipitation type (e.g. convective or stratiform) and the local variability in geophysical fields (such as surface type, soil texture, and topography). Even for a soil moisture network, the spatial extent of ground observations may not always represent the satellite footprint area since the latter varies over time. These factors pose an obstacle to validating satellite soil moisture products, especially when using the root-mean-square error (RMSE) metric.

Although point measurements are not readily converted to the spatial averages, the temporal variability of soil moisture observed by point measurement may be spatially representative (e.g. Brocca, Melone, Moramarco, & Morbidelli, 2009; Loew & Mauser, 2008; Martinez-Fernandez & Ceballos, 2005). Fig. 2 presents the soil moisture time sequences observed at four pairs of neighboring sites (all from MAWN). Each pair of sites may lie within the same SMOS footprint area. Although the absolute magnitudes of soil moisture are not necessarily matched, each pair of sites typically show good agreement for the temporal pattern of soil moisture. Likewise, at the Borden station soil moisture measurements taken at two locations are not always same in magnitude but showing consistent temporal dynamics for the period of record (not shown). Regarding the SCAN measurements, Liu et al. (2011) suggested that the SCAN point observations were highly correlated with the watershed average soil moisture obtained from network measurements and thus were suitable for evaluating the assimilation estimates with the correlation metric. Thus, overall the point-scale measurements (from MAWN, SCAN, and Borden) being used in this work are assumed to represent the areal average (satellite product scale or model grid cell) in terms of the temporal variability of soil moisture.

Since the absolute magnitude of soil moisture for the areal average (corresponding to the satellite footprint scale) is difficult to estimate based upon point-source observations, the SMOS retrievals are not validated with the RMSE metric in this study. Instead, we only assess the SMOS soil moisture skill R, which is defined as the daily time series correlation of SMOS retrievals with point measurements. SMOS measures only the water content within the top ~5–6 cm soil layer. Although the 5 cm depth matches well with the average soil penetration of SMOS, here the SMOS soil moisture skill is computed using in situ measurements taken at 10 cm depth or in the top 30 cm profile (for those sites with the vertically installed probes), to be consistent with the subsequent assessment of the model surface soil moisture skill (Sections 4.2 and 4.3). Overall the use of 10 cm-depth and 0–30 cm measurements is acceptable in this study since typically the time patterns of soil moisture between in situ measurements taken at 5 cm, 10 cm, and 20/25 cm are highly correlated.

To be consistent with the subsequent 1D-EnKF (Section 4), the SMOS retrievals (from both ascending and descending orbits) are mapped onto the MESH model grid cells (at a 1/6th degree resolution) using a nearest neighbor approach. Given a model grid, the SMOS skill (daily time series correlation R with in situ data) is assessed using in situ measurements falling within the grid cell. Typically only one in situ site is available per model grid cell. We do not compute the R values when any of the following occurs: (1) the effective length of SMOS soil moisture daily time series is less than 60 days per year; (2) in situ soil moisture (unfrozen) time series are shorter than 100 days per year; (3) the time series standard deviation of in situ soil moisture is less than 0.02 m^3/m^3 (since the measurement noise may significantly impact the R values when the time series standard deviation is too small); or (4) linear or quadratic trends in the SMOS or in situ time series significantly contribute to the correlation (by examining if a linear regression and a polynomial of the 2nd degree give statistically significant trends). Eventually, the skill R is computed for about 38 grids (per year).

Fig. 3 shows the SMOS soil moisture skill. To be consistent with the subsequent validation of the assimilation estimates, we classify the model grid cells into four types: (1) sCmC: the SMOS soil moisture has a nominal (low vegetation) surface type (the retrieval case value is 12 in MIR_SMUDP2; in this study, for the grids of interest, a nominal surface is typically a crop surface) and the crop cover is also dominant (>50%) within the model grid square; (2) sCmF: the SMOS soil moisture is from a crop surface node, but the fraction of forest cover (the sum of the deciduous, coniferous, and mixed forest classes) within the model grid cell exceeds 50% (note that since a model grid square and the SMOS node mapped onto the grid are not exactly matched in space their surface types may be not always the same); (3) sFmC: the SMOS retrieval mapped onto a model grid is from a forest surface node (the retrieval case values equals 11 in MIR_SMUDP2), but the model grid is dominated by crop cover; and (4) sFmF: the SMOS retrieval case is a forest surface and the model grid is also covered dominantly by forest. Table 1 provides the median and mean skill R for each grid type.

The SMOS retrievals from crop surfaces, i.e., at the sCmC and sCmF grids (triangles and diamonds in Fig. 3), typically show modest to high skill R (median of 0.55 for sCmC and 0.64 for sCmF), which means that the time variation of SMOS soil moisture at these grids agrees well with the temporal pattern of in situ measurements. In contrast, the SMOS observation skill is usually low at the sFmC and sFmF grids (squares and circles) where the retrievals come from forest cover-dominated surfaces (with a median of 0.23 for sFmC and 0.32 for sFmF). The identified SMOS skill disparity between forest and crop

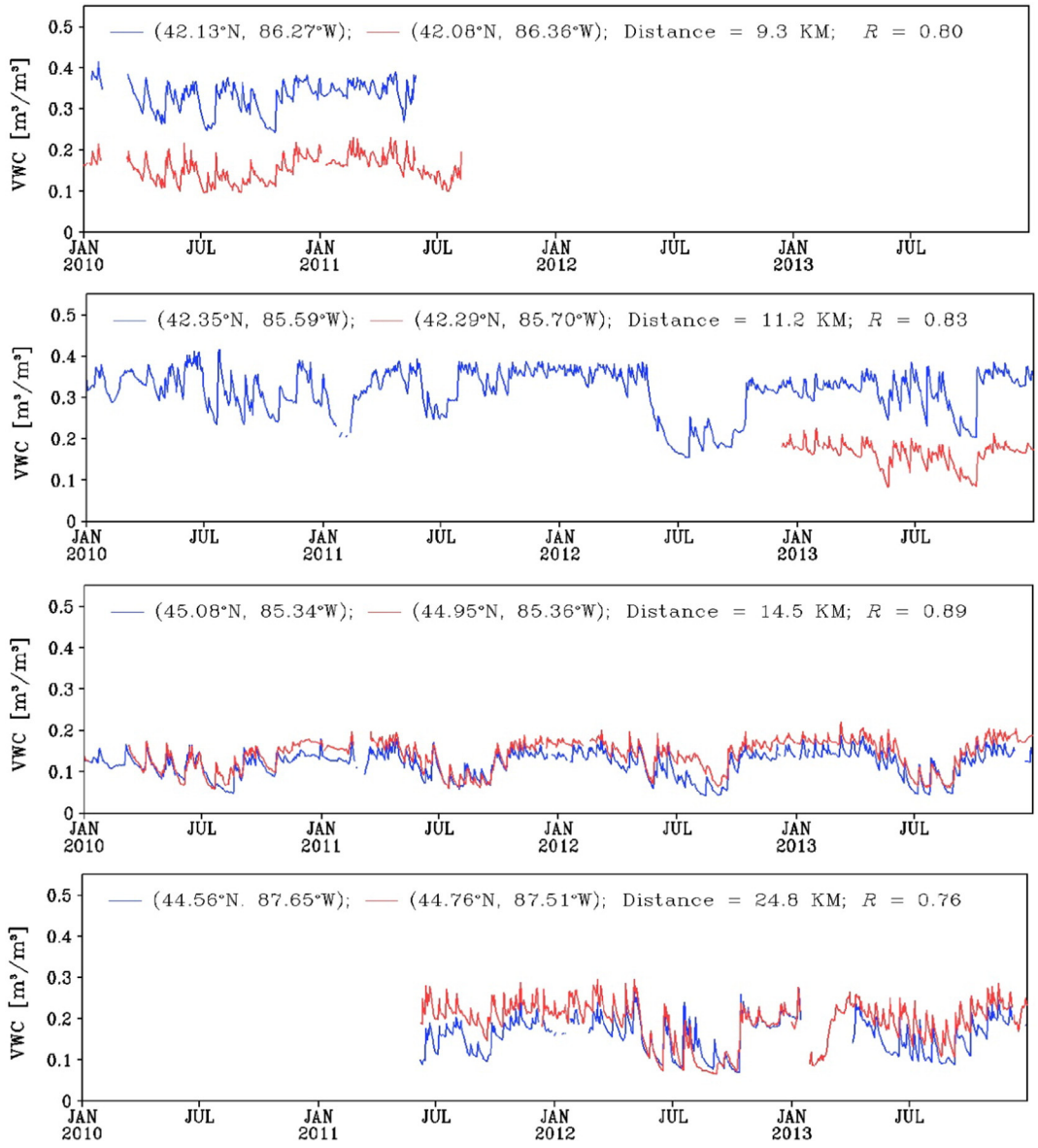

Fig. 2. Comparison of volumetric water content (VWC) daily time sequences for four pairs of MAWN sites. For each panel, location of the two sites and their distance are shown, and R denotes the correlation coefficient between the two soil moisture sequences. The labels on the x-axis denote the first day of each month.

surfaces is consistent with the fact that the satellite retrieval capabilities decrease with increased canopy density. Additionally, the forest grids with low SMOS skill are typically located near the lakes. The corresponding SMOS retrievals may also be impacted by the presence of open water and a low quality of the reconstructed brightness temperatures caused by the Gibbs effect (Gibbs, 1899) over the coast. Al Bitar et al. (2012) suggested that the temporal dynamics of soil moisture between SMOS and SCAN/SNOTEL point stations were typically well matched, but negatively affected by the increasing forest and/or water fractions within the satellite node. Note that such a vegetation modulation of the SMOS observation skill can strongly impact the model soil moisture skill gain through data assimilation (Sections 4.2 and 4.3).

4. Assimilation of SMOS soil moisture

A 1D-EnKF (i.e., the analysis increment computation is performed independently for the model grids) with 12 ensemble members is applied to assimilate SMOS retrievals into the MESH model. Given a model grid, in the EnKF analysis Eq. (1) the model state vector x_j (dimension is 21) is comprised of the volumetric liquid water content from all the seven GRUs within the grid cell and all the three soil layers modeled in MESH. The observation y_j is the perturbed SMOS soil moisture and the corresponding model prediction Hx_j^- denotes the model estimates of the grid-averaged volumetric liquid water content (a weighted sum of GRU values) in the model surface layer (0–10 cm). The assimilation period is from 1 January 2010 through 31 December 2013. The model is spun up for a 8-year period with the 2002–2009 forcing data.

In the EnKF, the estimates of the model forecast errors are derived from an ensemble of model integrations. To represent random errors in the forcing inputs, cross-correlated forcing perturbation fields are generated following Reichle et al. (2007). The selected perturbation parameters are largely based upon order-of-magnitude considerations (Reichle et al., 2002). To account for the model forecast errors due to deficiency in model physics and/or parameters, temporally correlated error perturbations are applied to soil moisture (volumetric liquid water content) estimates in the model. The following equation is used to yield the time evolution of error perturbations.

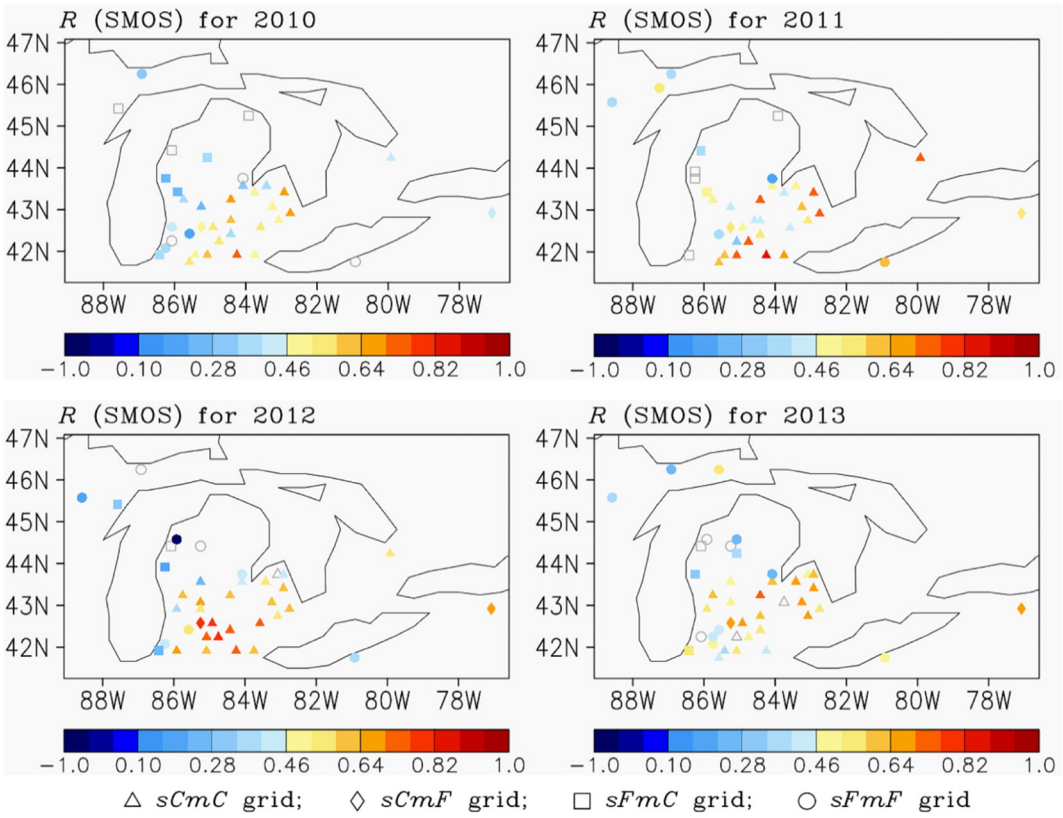

Fig. 3. SMOS soil moisture skill, which is defined as the correlation coefficient *R* of daily averaged SMOS retrievals with in situ measurements, over four individual years. *R* is computed after the SMOS retrievals are mapped onto the model grid coordinate system. Symbols indicate the model grid types as defined in the text: (triangles) sCmC, (diamonds) sCmF, (squares) sFmC, and (circles) sFmF. *R* values that are not significantly (5% level) different from zero are indicated by open symbols in gray.

$$q_k = \sigma\left[(1-k/\tau)w_0 + \sqrt{1-(1-k/\tau)^2}\,w_k\right] \quad (2)$$

where q is the error perturbation ensemble, w is white noise ensemble with mean of 0 and variance of 1, τ is the correlation time length (unit: the model time step), k denotes the time index ($0 \le k < \tau$), and σ represents the specified model error standard deviation. Currently, the 0.001 m^3/m^3, 0.0005 m^3/m^3, and 0.00005 m^3/m^3 error standard deviations are applied to the model's three layers (0–10, 10–35, and 35–410 cm), respectively. The model error correlation time is set to 1 day, which is the approximate frequency for the SMOS observations (1 or 2 observations every 3 days for both ascending and descending passes). In the EnKF, the measurement errors are represented using another ensemble with the mean equal to zero and the variance equal to the observation error variance. In this study, a uniform error standard deviation of 0.08 m^3/m^3 (derived from the SMOS climatology) is assumed for the SMOS retrievals. Although the input error parameters are not on-line tuned in our assimilation, Reichle, Crow, and Keppenne (2008) demonstrates that a non-adaptive EnKF typically performs well for soil moisture estimates, even when the input error parameters moderately deviate from their true values. However, when the error estimates for the model and/or the retrievals are far from the realistic conditions, the assimilation estimates may be even worse than the open-loop (Reichle, Crow, and Keppenne, 2008).

4.1. Bias detection and reduction

If we directly assimilate the unscaled SMOS soil moisture product, the analysis (updating the model forecast with a SMOS observation) typically makes systematic corrections to the model estimate. Negative mean increments (change in the model estimate between after and before the updating) are pronounced across the study region for both the

Table 1
Median and mean skill *R* within each grid type for soil moisture from SMOS, the open-loop model, and the assimilation, respectively.

Soil layer	Grid type	*N*	Median *R*			Mean *R* with 95% confidence intervals		
			SMOS	Open-loop	Assim.	SMOS	Open-loop	Assim.
0–10 cm	sCmC	91	0.55	0.39	0.64	0.55 ± 0.01	0.39 ± 0.01	0.64 ± 0.01
	sCmF	8	0.64	0.60	0.74	0.62 ± 0.04	0.61 ± 0.03	0.73 ± 0.02
	sFmC	21	0.23	0.40	0.52	0.23 ± 0.04	0.42 ± 0.02	0.50 ± 0.02
	sFmF	33	0.32	0.62	0.60	0.29 ± 0.03	0.60 ± 0.02	0.61 ± 0.02
0–35 cm	sCmC	89	–	0.51	0.72	–	0.47 ± 0.01	0.71 ± 0.01
	sCmF	8	–	0.65	0.80	–	0.67 ± 0.03	0.77 ± 0.02
	sFmC	20	–	0.49	0.54	–	0.48 ± 0.02	0.53 ± 0.02
	sFmF	32	–	0.67	0.65	–	0.64 ± 0.02	0.62 ± 0.02

Grid types are defined in the text. *N* denotes the combined number of grid-based *R* values for 2010–2013.

surface layer and the root zone (not shown here). This provides clear evidence of the presence of bias in the system. If the system is bias-free (i.e., no systematic errors in either the model or the SMOS observation), mean analysis increments should be close to zero. This bias problem was also indicated by non-zero mean innovations and non-zero difference between climatology of satellite retrievals and that of their model equivalents.

Data assimilation systems are usually designed to produce an optimal estimate based upon the hypothesis of unbiased (and uncorrelated) errors in model and observation (i.e., a bias-blind system). In practice, biases in model forecast or observation (including observation operator) would contribute to the error variances, resulting in a suboptimal analysis. Observation biases, if present and known, should be removed prior to the assimilation. Provided that we can attribute the systematic errors to proper sources, and they also can be represented, by design, using appropriate parameters, the biases can be estimated jointly with the model state by adding the designed parameters to the state vector (i.e., a bias-aware system). However, this is extremely complicated to achieve considering limited reference data and thus beyond the scope of this work.

Following previous studies (e.g., Draper et al., 2012; Liu et al., 2011; Reichle & Koster, 2004; Reichle et al., 2007) we utilize a bias reduction scheme that matches the cumulative distribution function (CDF) of SMOS retrievals to the MESH model surface soil moisture's CDF by scaling the retrievals. The CDF matching scheme can effectively remove the climatological difference (mean and standard deviation) between satellite retrievals and model data, with little impact on the SMOS soil moisture skill. The skill for the rescaled SMOS retrievals is almost identical to the skill of unscaled SMOS (Fig. 3). However, notice that since the absolute magnitude of SMOS soil moisture is changed the assimilation products are meaningful only in terms of the time variability of soil moisture, which is consistent with the advantage of point measurements (Section 3). In the present study, the model CDF is based on the 4-year (2010–2013) model surface soil moisture, while the SMOS soil moisture CDF (and the scaling of SMOS) is calculated separately for 2010/2011 and 2012/2013 since there are non-negligible inconsistencies in SMOS retrievals between the two periods (due to the change of the dielectric constant model in the retrieval algorithms). Correspondingly, the SMOS observation error standard deviation (0.08 m^3/m^3) is rescaled by multiplying it with the ratio between the scaled SMOS time series standard deviation (very close to the model soil moisture standard deviation) and the unscaled SMOS time series standard deviation. The rescaling of the SMOS retrievals and their error standard deviations is conducted locally. In addition, we also matched the satellite and model CDFs separately for the two model periods (2010–2011 and 2012–2013) and independently for each season. Results indicated that the rescaling parameters depended only weakly upon the model period and the season for this study.

4.2. Skill improvement over open-loop

Fig. 4 compares the surface soil moisture skills from the open-loop model (single integration without assimilation) and the assimilation estimates based upon the scaled SMOS retrievals. Here the surface soil moisture skill refers to the correlation R (daily time series) between the grid-averaged soil moisture from the model surface layer (0–10 cm) and in situ measurements taken at 10 cm depth or in the 0–30 cm profile (the probe is vertically installed for some sites). R values are not computed if the length of SMOS and/or in situ soil moisture time series is short or when the correlation is strongly affected by the in situ measurement noise or the trends (Section 3). Consistent with the assessment of the SMOS skill, the model grids are categorized as the sCmC, sCmF, sFmC, and sFmF types (Section 3). Table 1 summarizes the median and mean skill R within each grid type for each soil moisture product.

To test the significance of the difference between skills for the three soil moisture products (SMOS, the open-loop, and the assimilation), the Fisher Z transform method is used. Assuming that two correlations R_1 and R_2 are independent, the Z-score for the difference between the two correlations can be expressed as (Dunn & Clark, 1969; Meng, Rosenthal, & Rubin, 1992)

$$z = \frac{\left(0.5\, ln\frac{1+R_1}{1-R_1}\right) - \left(0.5\, ln\frac{1+R_2}{1-R_2}\right)}{\sqrt{\frac{1}{N_1-3}+\frac{1}{N_2-3}}} \tag{3}$$

where N_1 and N_2 are the sample sizes for R_1 and R_2. Given a significance level, the two correlations are statistically different from each other if the absolute Z-score exceeds the corresponding critical value. In practice, the assumption that the correlations (skills) are independent is not strictly valid for the three soil moisture products. To this end, the significance was estimated using a Monte Carlo approach for a limited number of grids (due to computational burden). This preliminary test confirmed the results assuming independence very closely approximate the Monte Carlo-based results. Thus, all statistical tests for the skill difference reported in the paper utilize the independence assumption and are not Monte Carlo based.

The open-loop model (Fig. 4, left column) typically provides higher surface soil moisture skill R at the sFmF and sCmF grids (median/mean of about 0.61), which are covered dominantly by forest, than at the sCmC and sFmC grids (median/mean of about 0.40) that are dominated by crop cover. Through the assimilation, the four grid types experience different skill gains $\Delta R^{A\text{-}M}$, defined as the skill for the assimilation soil moisture product minus the skill for the open-loop estimates (Fig. 4, right). Overall the sCmC grids (triangles) have the largest improvement $\Delta R^{A\text{-}M}$, and the sFmF grids (circles) show the weakest or even negative $\Delta R^{A\text{-}M}$; while soil moisture from the sCmF and sFmC grids (diamond and square signs) typically shows low to modest increase in skill. The skill gain $\Delta R^{A\text{-}M}$ is typically statistically significant for the sCmC grids. After the assimilation (Fig. 4, middle), the surface soil moisture skill R for the sCmC grids (median/mean of about 0.64) are typically closer to or even larger than R for the forest-dominated grids (sCmF and sFmF). Similarly, Draper et al. (2012) revealed larger skill (anomaly R) improvements for the cropland than for the mixed cover class (10–60% trees or woody plants) when assimilating the AMSR-E and ASCAT retrievals in the Catchment Land Surface Model (CLSM).

The counterpart of Fig. 4 for root-zone soil moisture (0–35 cm) is provided in Fig. 5. The root-zone soil moisture skill is derived using a depth-weighted average of soil moisture estimates in the model's top two layers (0–10 and 10–35 cm) against the arithmetic mean of in situ measurements at 10 and 25 cm depths or the 0–30 cm profiles measured by vertically installed sensors. The variations with the grid types of the open-loop skill and the skill gain $\Delta R^{A\text{-}M}$ for root-zone soil moisture are quite similar to those observed for the surface soil moisture. Overall the open-loop skill for root-zone soil moisture (Fig. 5, left column) is higher at forest-dominated grids (sFmF and sCmF) than at crop cover-dominated grids (sCmC and sFmC). The strongest skill improvement $\Delta R^{A\text{-}M}$ for root-zone soil moisture are also observed for the sCmC grids (triangles in Fig. 5, right). This clearly indicates that the surface soil moisture information measured by SMOS, through the EnKF assimilation, can be propagated to the soil layers that are not directly measured. For a given grid type, on average, the skill for root-zone soil moisture is slightly higher than the surface soil moisture skill (for both the open-loop and the assimilation product) (Table 1).

The skill improvement $\Delta R^{A\text{-}M}$ is controlled not only by the satellite observation skill but also by the skill for the open-loop estimates. In general, the skill improvement $\Delta R^{A\text{-}M}$ increases as the satellite observation skill, but decreases with increased open-loop skill (Reichle, Crow, Koster, Sharif, & Mahanama, 2008). Therefore, when the satellite observation skill is high and the model (open-loop) skill is low, the largest

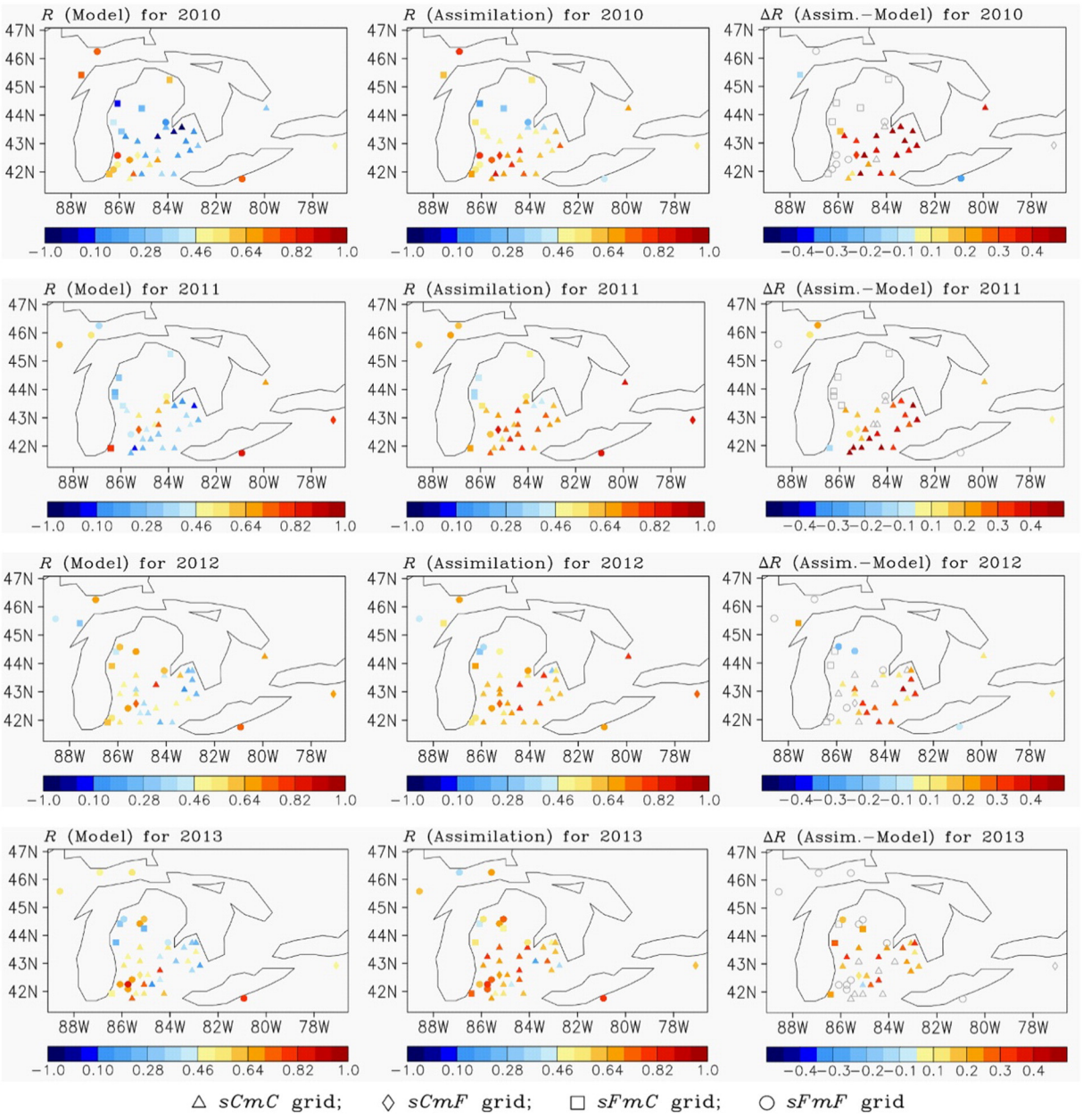

Fig. 4. Skill for surface soil moisture (0–10 cm) from (left) the open-loop model and (middle) the assimilation, and (right) the skill improvement $\Delta R^{A\text{-}M}$ (Assimilation minus Open-loop) over four individual years (top to bottom: 2010, 2011, 2012, and 2013). In the right column, $\Delta R^{A\text{-}M}$ is denoted by an open symbol in gray if the open-loop R and the assimilation R are not significantly (5% level) different from each other. Symbols denote the model grid types, same as in Fig. 3.

skill improvement $\Delta R^{A\text{-}M}$ is expected, which typically corresponds to the sCmC case. On the contrary, if the satellite observation skill is low and the open-loop model skill is high, we usually expect weak $\Delta R^{A\text{-}M}$, as observed for the sFmF grids. When the satellite skill and the open-loop skill are either both high (e.g. sCmF grids) or both low (e.g. sFmC grids), $\Delta R^{A\text{-}M}$ are typically low to modest.

The skill improvement $\Delta R^{A\text{-}M}$ (the assimilation skill minus the open-loop skill) against $\Delta R^{S\text{-}M}$, defined as the SMOS observation skill minus the skill for the open-loop surface soil moisture, is provided in Fig. 6. Overall the skill improvement $\Delta R^{A\text{-}M}$ for both surface and root-zone soil moisture (the ordinate) is strongly related to $\Delta R^{S\text{-}M}$ (the abscissa). Every time the SMOS skill is greater than or equal to the open-loop surface soil moisture skill, the assimilation is typically able to significantly improve the skill of the model estimates. Such is the case with most of the sCmC grids (triangles). When the satellite observation skill is about 0–0.3 lower than the open-loop model (i.e., $\Delta R^{S\text{-}M}$ along the abscissa is between −0.3 and 0), the open-loop skill was still improved by the assimilation for most cases (85% for surface soil moisture and 80% for root-zone soil moisture), but the improvements are not always statistically significant. If the skill for SMOS retrievals is more than about 0.3 below the open-loop skill (i.e., $\Delta R^{S\text{-}M}$ is less than −0.3), the assimilation is not helpful and even negatively affects the open-loop skill. The results are fairly consistent with Draper et al. (2012). The study showed that the assimilation of AMSR-E and ASCAT retrievals in CLSM typically generated an improved skill (in terms of anomaly R) for both the surface and root zone soil moisture as long as the satellite observation skill is no more than about 0.2 lower than the open-loop skill.

For the retrievals of very low or even negative skill ($\Delta R^{S\text{-}M}$ is thus small in Fig. 6), which generally reflect poor satellite observations, their real errors could be severely underestimated by the input error parameters, thus causing negative $\Delta R^{A\text{-}M}$. Overall, negative $\Delta R^{A\text{-}M}$ is severer in root zone than for the surface layer (Fig. 6). This is generally consistent with the finding that poorly specified observation errors have a fiercer impact on the assimilation estimates of root zone soil

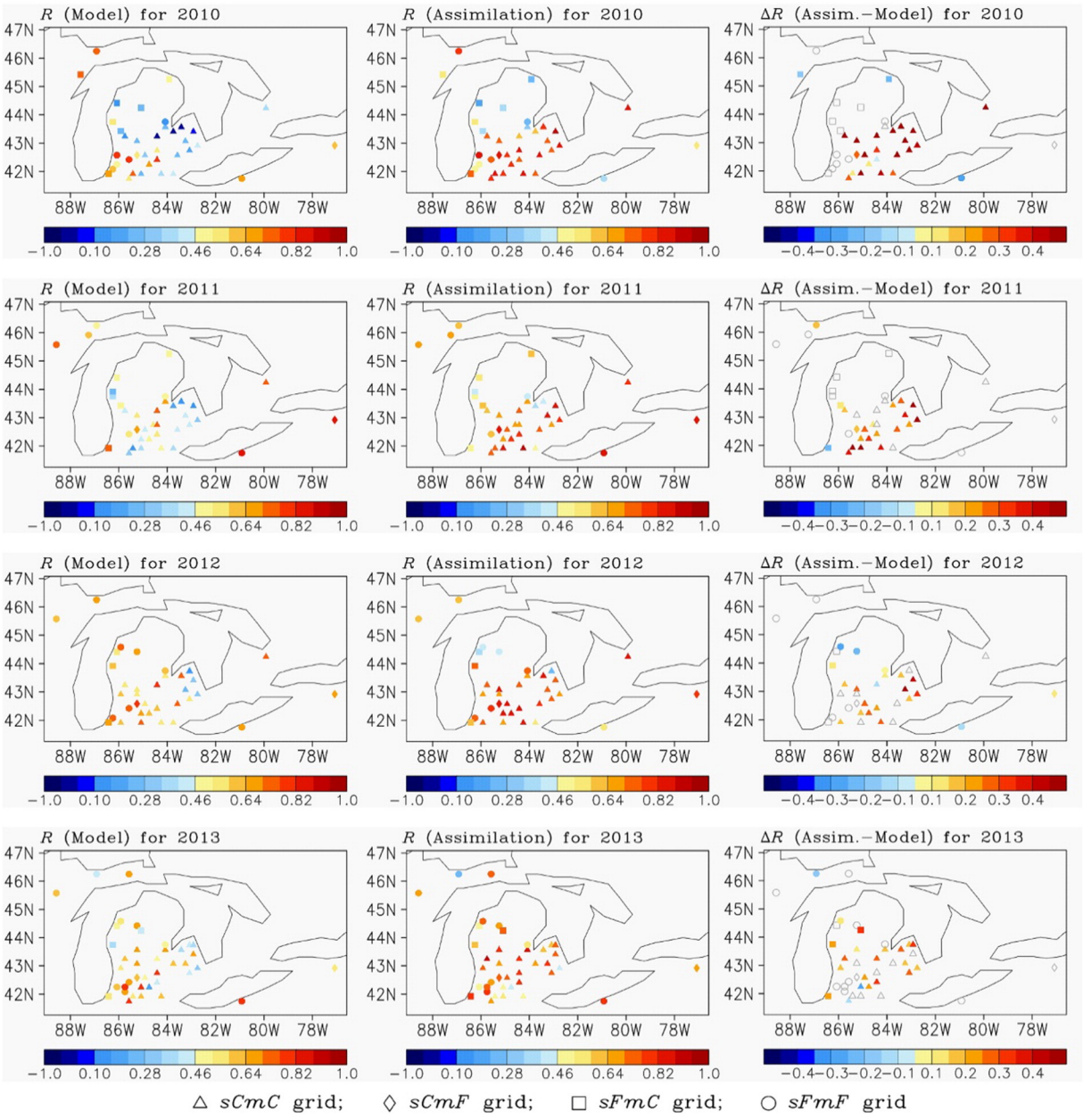

Fig. 5. Similar to Fig. 4, but for root-zone (top 35 cm) soil moisture.

moisture than on surface soil moisture estimates (Reichle, Crow, and Keppenne, 2008). The on-line quality control routines (e.g., Reichle, 2008) and on-line tuning of error covariances (Reichle, Crow, and Keppenne, 2008) may be helpful for controlling the occurrence of negative $\Delta R^{A\text{-}M}$. Note that although the assimilation skill does not necessarily exceed the skill of the open-loop model for individual grids, the assimilation product always outperforms or at least match the open-loop counterpart in terms of the averaged skill for each grid type (Table 1), coinciding with the finding based on synthetic assimilation experiments (Reichle, Crow, Koster, et al., 2008). Additionally, as shown in Fig. 6, overall the surface soil moisture $\Delta R^{A\text{-}M}$, relative to root-zone $\Delta R^{A\text{-}M}$, exhibits a better linear relationship with $\Delta R^{S\text{-}M}$. For a given $\Delta R^{S\text{-}M}$, the skill improvement $\Delta R^{A\text{-}M}$ is usually more variable (along the ordinate) for root-zone soil moisture than for surface soil moisture. This may be due to the fact that during the assimilation the updating of root-zone soil moisture is subject to the accurate information exchanges between the surface soil and the deeper layers, which, in turn, are controlled by many factors (e.g. the model dynamics and the input error parameters). However, notice that a perfect linear relationship between $\Delta R^{A\text{-}M}$ and $\Delta R^{S\text{-}M}$ is not expected since the sensitivity of $\Delta R^{A\text{-}M}$ to $\Delta R^{S\text{-}M}$ is additionally affected by the magnitude of open loop skill.

4.3. Skill improvement over SMOS

In theory, the assimilation seeks to produce superior estimates, relative to both the open-loop model and the observation product alone. In this section, we investigate the skill improvement, relative to the SMOS observation skill, by the assimilation. Fig. 7 shows $\Delta R^{A\text{-}S}$, defined as the skill for the surface soil moisture assimilation product minus the SMOS observation skill. It is expected that $\Delta R^{A\text{-}S}$, as opposed to $\Delta R^{A\text{-}M}$, increases as the open-loop skill (since the assimilation product skill typically increases with the open-loop skill for the same observation skill), but decreases with increased satellite observation skill. As expected, overall the variation of $\Delta R^{A\text{-}S}$ with the grid type (Fig. 7) is opposite to

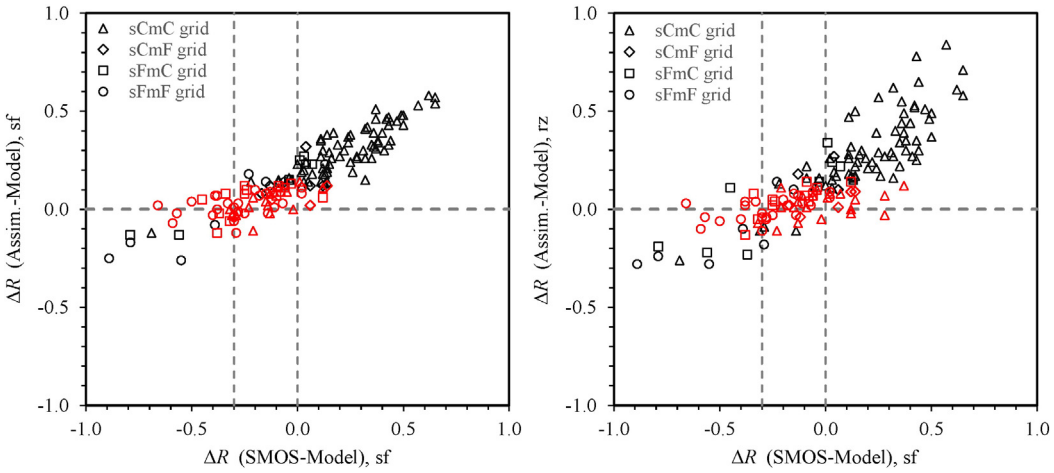

Fig. 6. Skill improvement $\Delta R^{A\text{-}M}$ (skill for the assimilation minus the open-loop skill, ordinate) for (left) surface and (right) root-zone soil moisture against $\Delta R^{S\text{-}M}$ (skill for the SMOS observation minus skill for the open-loop surface soil moisture, abscissa). Symbols indicate the model grid types as defined in the text: (triangles) sCmC, (diamonds) sCmF, (squares) sFmC, and (circles) sFmF. Symbols in red mean that $\Delta R^{A\text{-}M}$ are not statistically significant at the 5% level. The horizontal dashed line denotes $\Delta R^{A\text{-}M} = 0$. The two vertical dashed lines denote $\Delta R^{S\text{-}M} = -0.3$ and $\Delta R^{S\text{-}M} = 0$, respectively.

that for $\Delta R^{A\text{-}M}$ (Fig. 4, right column). At the sFmF and sFmC grids (circles and squares in Fig. 7), the surface soil moisture skill for the assimilation typically significantly exceeds the skill of SMOS product alone (but the corresponding $\Delta R^{A\text{-}M}$ is typically small or even negative, as discussed above). This is mainly because that for the two grid types the open-loop skill is typically much higher than the satellite skill (e.g. Table 1). In contrast, smaller $\Delta R^{A\text{-}S}$ are usually observed for the sCmC grids (triangles in Fig. 7; the corresponding $\Delta R^{A\text{-}M}$ is typically the strongest).

The SMOS observation skill could even exceed the assimilation skill at a few of the sCmC grids (Fig. 7). Reichle, Crow, Koster, et al. (2008), based upon synthetic experiments (Fig. 2a therein), also found that the surface soil moisture skill from the assimilation was not always above the satellite observation skill (anomaly R was used therein), especially in the presence of a poor open-loop model skill and a high satellite skill (such is the case with our sCmC grids showing negative $\Delta R^{A\text{-}S}$). As they pointed out, the reasons for the occurrence of negative $\Delta R^{A\text{-}S}$ may include the effects from the nonlinearity of the system, a small ensemble size, and the imperfect input error parameters, etc. However, note that overall the surface soil moisture assimilation skill (median/mean of 0.64) is still

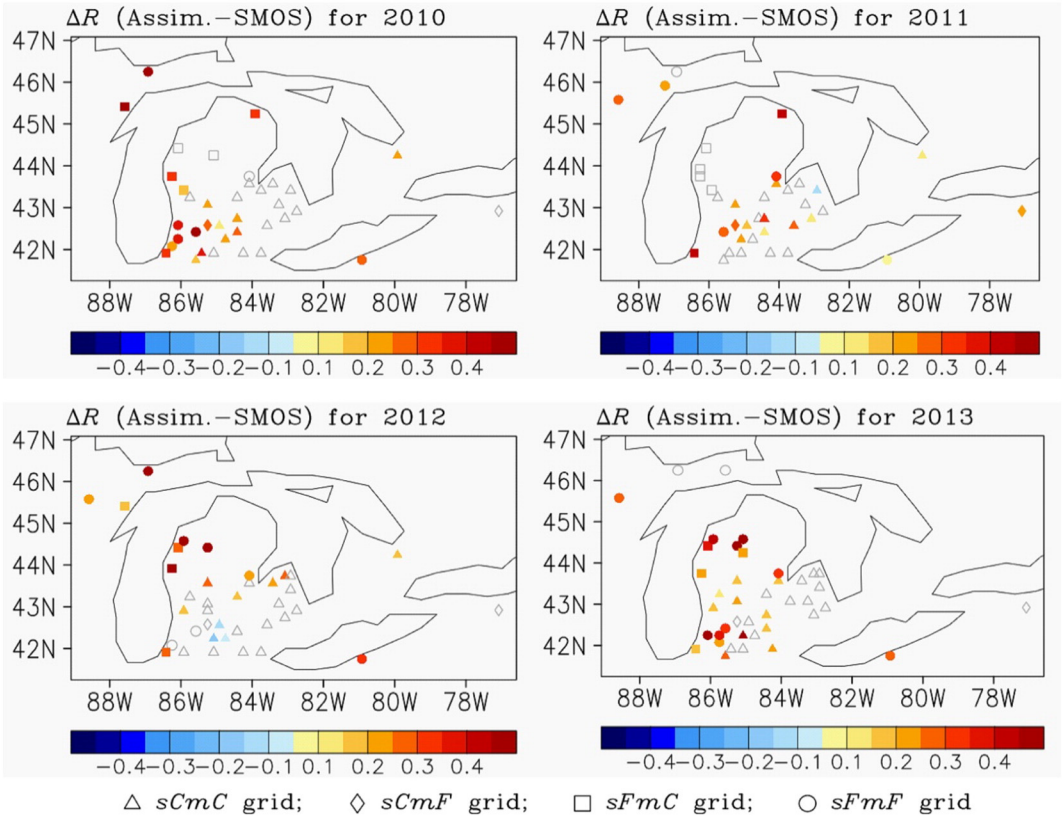

Fig. 7. Skill improvement $\Delta R^{A\text{-}S}$, defined as the skill for the surface soil moisture assimilation product minus the SMOS observation skill. $\Delta R^{A\text{-}S}$ in gray open symbol means that the assimilation skill and the SMOS skill are not significantly (5% level) different from each other. Symbols denote the model grid types, same as in Fig. 4.

significantly better than the SMOS product skill (median/mean of 0.55) for the sCmC-type grid (Table 1).

4.4. Subgrid-scale (GRU) soil moisture skill

In the above, point in situ measurements are used to assess the skill for the grid-scale soil moisture. It is acknowledged that there could be a mismatch in vegetation or soil characteristics between the two products with different spatial scales. A model grid square typically represents a mixture of multiple land cover and soil attributes, while a point station corresponds to only a specific vegetation and/or soil type. In this study, however, this factor is expected to have negligible effects on the skill evaluation above since the land cover type for in situ station is typically consistent with the dominant land cover class for the grid-scale soil moisture.

We also computed the subgrid-scale soil moisture skill, i.e., point measurements are compared with the model soil moisture from a subgrid area that has the same vegetation or soil characteristics as the point site. In the MESH model, the subgrid-scale variability is resolved using the GRU approach (Section 2.2). Each model grid cell is a mosaic of up to seven GRUs. Each GRU corresponds to one land cover class (other soil characteristics are assumed to be same for the same GRU type) and is weighted by the fraction of the land cover class within the grid cell. Hence, for a given grid location, the soil moisture skill for a specific GRU, which corresponds to the land cover class for the in situ station, is assessed. Overall the subgrid-scale (GRU) soil moisture (not shown) and the grid-averaged soil moisture reveal a consistent vegetation modulation of skill for both the open-loop and the assimilation. The open-loop model usually provides strong soil moisture skill for forest GRUs and weaker skill for crop GRUs. A crop GRU, if the SMOS soil moisture sampled from a crop surface node is assimilated, typically experiences a large skill improvement $\Delta R^{A\text{-}M}$. When the assimilated SMOS retrievals come from a forest-type surface, the skill improvement $\Delta R^{A\text{-}M}$ for the crop GRU soil moisture is relatively weak. The assimilation typically leads to smaller or even negative $\Delta R^{A\text{-}M}$ for forest-GRUs, even when the assimilated SMOS soil moisture is from a crop surface node. To further improve the assessment of the soil moisture skill, dense in situ observations would clearly be of advantage, although such data are not available for this study.

5. Summary and discussion

Since the launch of SMOS satellite mission, the validation and assimilation of SMOS soil moisture has been an active research area. In this paper, the 1D-EnKF is applied to assimilate SMOS soil moisture retrievals into the MESH model over the Great Lakes basin. The satellite retrievals, the open-loop soil moisture, and the assimilation estimates are validated against point-scale in situ soil moisture measurements from MAWN, SCAN and FCRN, in terms of the daily time series correlation coefficient (soil moisture skill R). Due to the bias between the SMOS retrievals and the model soil moisture estimates, a priori rescaling on the retrievals is performed using the CDF matching. Our focus in this work is thus on the assimilation of the scaled SMOS retrievals. The main results from this study are as follows.

(1) The observation skill is typically low for the SMOS retrievals from forest surface nodes, but becomes high for those from crop surfaces, consistent with the effect of canopy density on the satellite retrieval capabilities. On the other hand, the open-loop model typically provides higher soil moisture skill R over forests than over crops.

(2) Overall the assimilation can favorably influence the model soil moisture skill for both the surface layer and the root zone except for the cases with a small SMOS observation skill and a large open-loop skill. The skill improvement $\Delta R^{A\text{-}M}$, defined as the skill for the assimilation soil moisture product minus the skill for the open-loop estimates, for both surface and root-zone soil moisture typically increases as the SMOS observation skill and decreases with increased open-loop skill, showing a strong linear relation to $\Delta R^{S\text{-}M}$, defined as the SMOS observation skill minus the open-loop surface soil moisture skill. When the SMOS skill is greater than or equal to the open-loop surface soil moisture skill, the assimilation is typically able to significantly increase the open-loop soil moisture skill.

(3) The crop-dominated grids typically experience the largest $\Delta R^{A\text{-}M}$ if the assimilated SMOS retrievals also come from crop surfaces, consistent with a high satellite observation skill and a low open-loop skill, while $\Delta R^{A\text{-}M}$ is usually the weakest for the forest-dominated grids when the SMOS retrievals from forest surfaces are assimilated, due to a low observation skill and a high open-loop skill.

(4) On average, the skill for the surface soil moisture assimilation product is always significantly better than the skill for the SMOS product alone, although the dependence of $\Delta R^{A\text{-}S}$ (skill for the surface soil moisture assimilation product minus the SMOS observation skill) upon the open-loop skill and the satellite observation skill is opposite to that for $\Delta R^{A\text{-}M}$. The forest-dominated grids, if the assimilated SMOS retrievals also come from forest surfaces, typically have large $\Delta R^{A\text{-}S}$ because the corresponding open-loop skill is generally higher than the satellite skill. In contrast, smaller $\Delta R^{A\text{-}S}$ are typically observed when the assimilated SMOS retrievals are from crop surfaces since the corresponding SMOS observation skill is high.

(5) We also investigated the subgrid-scale (GRU) soil moisture skill by comparing point measurements with the GRU soil moisture (a GRU and an in situ site lie within the same grid cell and have the same land cover class). Overall the GRU soil moisture skill and the grid-scale soil moisture skill show a consistent vegetation modulation for both the open-loop and assimilation estimates. This confirms a negligible impact of point measurements (in situ data) on the skill assessment for the grid-scale soil moisture (the model and SMOS) due to the possible disparity in vegetation characteristics between them.

Unlike previous assimilation studies of SMOS soil moisture (e.g. Ridler et al., 2014; Zhao et al., 2014), this work assimilated 4 years of SMOS retrievals (2010–2013) at a grid scale of ~15 km. The overall agreement within the same grid type and the overall consistency between the years are observed for each of the three soil moisture products (SMOS, the open-loop, and the assimilation), which demonstrates the robustness of our results. This study also suggests that the ability of SMOS/MIRAS to measure surface soil moisture for a wide range of vegetation covers is clearly of advantage for assessing the vegetation modulation of the assimilation. The results offer further insight into the dependence of the assimilation upon the open-loop skill and the satellite observation skill.

In this work, only the correlation R metric of skill is used to assess the three data sets (SMOS alone, the open-loop model, and the assimilation estimates) because (1) the temporal variability of soil moisture (rather than the absolute magnitude) observed by point measurements is spatially representative; and (2) the absolute magnitude of the soil moisture assimilation product is meaningless since the satellite retrievals are rescaled prior to the assimilation (Reichle et al., 2007). Note that through a percentile-based transformation (e.g., Entekhabi, Reichle, Koster, & Crow, 2010) the time variations of soil moisture can be scaled to the soil moisture initial conditions of weather and climate models, while any bias (systematic error) in the soil moisture product can be scaled out (e.g. Zhang & Frederiksen, 2003). Therefore, the resulting soil moisture assimilation product can benefit weather and climate forecast initializations as long as the time variability of soil moisture is captured accurately. The skill R values presented in this work are derived

based upon the original soil moisture time series. To assess the impact of soil moisture seasonality on the skill *R* estimates, we also analyzed the anomaly *R*. The soil moisture anomalies are defined as departures of daily soil moisture from the seasonal (monthly mean) climatology (e.g., Reichle et al., 2007). At least three years of complete estimates, for each soil moisture product, are required for extracting the soil moisture seasonal climatology. In addition, for a given grid, a minimum of 60-day SMOS anomalies and 100-day in situ anomalies (per year) are required for computing the anomaly *R*. Eventually, only 18 grids are available for the anomaly *R* analysis. Overall our *R* metric of skill (based upon the original time series) and the anomaly *R* metric lead to the consistent general conclusions.

In the present work, overall the open loop soil moisture skill for 2010/2011 is lower than that for 2012/2013 (Figs. 4 and 5). The difference may be caused by two sources: (i) the meteorological forcing data (notably rainfall) used for 2010/2011 may be in relatively low quality; and (ii) the model parameters (related to physiography, vegetation, and soil characteristics), which were based upon a calibration with the 2004–2005 streamflow observations (Haghnegahdar et al., 2014), may be not the "best" for 2010/2011. If the improved forcing data and/or calibrated model parameters are applied, the 2010/2011 open-loop skill could be increased and the corresponding skill improvement through the assimilation is expected to decrease (as shown for 2012/2013). However, our general conclusions remain valid.

Supplementary data to this article can be found online at http://dx.doi.org/10.1016/j.rse.2015.08.017.

Acknowledgment

We are grateful to the ESA and the ESA Earth Observation Missions Helpdesk Team for providing the SMOS soil moisture product, and to the MAWN (Michigan State University and the Enviro-weather project) and the Natural Resources Conservation Service (NRCS) for their in situ soil moisture data used in this study. The lead author is generously supported through an NSERC (CGSD3-403498-2011) CGSD and a Meteorological Service of Canada Graduate Supplement Scholarship.

References

Al Bitar, A., Leroux, D., Kerr, Y.H., Merlin, O., Richaume, P., Sahoo, A., et al. (2012). Evaluation of SMOS soil moisture products over continental U.S. using the SCAN/SNOTEL network. *IEEE Transactions on Geoscience and Remote Sensing, 50*, 1572–1586.

Albergel, C., de Rosnay, P., Gruhier, C., Muñoz-Sabater, J., Hasenauer, S., Isaksen, L., et al. (2012). Evaluation of remotely sensed and modelled soil moisture products using global ground-based in situ observations. *Remote Sensing of Environment, 118*, 215–226.

Brocca, L., Melone, F., Moramarco, T., & Morbidelli, R. (2009). Soil moisture temporal stability over experimental areas of Central Italy. *Geoderma, 148*(3–4), 364–374. http://dx.doi.org/10.1016/j.geoderma.2008.11.004.

Brocca, L., Melone, F., Moramarco, T., Wagner, W., Naeimi, V., Bartalis, Z., et al. (2010). Improving runoff prediction through the assimilation of the ASCAT soil moisture product. *Hydrology and Earth System Sciences, 14*, 1881–1893.

Crow, W.T., Berg, A.A., Cosh, M.H., Loew, A., Mohanty, B.P., Panciera, R., et al. (2012). Upscaling sparse ground-based soil moisture observations for the validation of coarse-resolution satellite soil moisture products. *Reviews of Geophysics*, *50*, RG2002. http://dx.doi.org/10.1029/2011RG000372.

Crow, W.T., Bindlish, R., & Jackson, T.J. (2005). The added value of spaceborne passive microwave soil moisture retrievals for forecasting rainfall-runoff ratio partitioning. *Geophysical Research Letters*, *32*, L18401. http://dx.doi.org/10.1029/2005GL023543.

Crow, W.T., & Wood, E.F. (2003). The assimilation of remotely sensed soil brightness temperature imagery into a land surface model using Ensemble Kalman filtering: A case study based on ESTAR measurements during SGP97. *Advances in Water Resources, 26*, 137–149.

Crow, W., & Zhan, X. (2007). Continental-scale evaluation of remotely sensed soil moisture products. *IEEE Geoscience and Remote Sensing Letters, 4*(3), 451–455. http://dx.doi.org/10.1109/LGRS.2007.896533.

Draper, C.S., Reichle, R.H., De Lannoy, G.J.M., & Liu, Q. (2012). Assimilation of passive and active microwave soil moisture retrievals. *Geophysical Research Letters*, *39*, L04401. http://dx.doi.org/10.1029/2011GL050655.

Drusch, M. (2007). Initializing numerical weather prediction models with satellite-derived surface soil moisture: Data assimilation experiments with ECMWF's Integrated Forecast System and the TMI soil moisture data set. *Journal of Geophysical Research*, *112*, D03102. http://dx.doi.org/10.1029/2006JD007478.

Dunn, O.J., & Clark, V.A. (1969). Correlation coefficients measured on the same individuals. *Journal of the American Statistical Association, 64*, 366–377.

Entekhabi, D., Reichle, R.H., Koster, R.D., & Crow, W.T. (2010). Performance metrics for soil moisture retrievals and application requirements. *Journal of Hydrometeorology*, *11*, 832–840.

Evensen, G. (1994). Sequential data assimilation with a non-linear quasigeostrophic model using Monte-Carlo methods to forecast error statistics. *Journal of Geophysical Research, 99*(C5), 10143–10162.

Evensen, G. (2003). The Ensemble Kalman Filter: theoretical formulation and practical implementation. *Ocean Dynamics*, *53*, 343–367.

Gherboudj, I., Magagi, R., Goita, K., Berg, A.A., Toth, B., & Walker, A. (2012). Validation of SMOS data over agricultural and boreal forest areas in Canada. *IEEE Transactions on Geoscience and Remote Sensing, 50*, 1623–1635.

Gibbs, J.W. (1899). Fourier's series. *Nature*, *59*, 606. http://dx.doi.org/10.1038/059606a0.

Haghnegahdar, A., Tolson, B.A., Davison, B., Seglenieks, F.R., Klyszejko, E., Soulis, E.D., et al. (2014). Calibrating Environment Canada's MESH Modelling System over the Great Lakes Basin. *Atmosphere-Ocean*, *52*, 281–293. http://dx.doi.org/10.1080/07055900.2014.939131.

Jackson, T.J., Bindlish, R., Cosh, M.H., Tianjie, Z., Starks, P.J., Bosch, D.D., et al. (2012). Validation of soil moisture and ocean salinity (SMOS) soil moisture over watershed networks in the U.S. *IEEE Transactions on Geoscience and Remote Sensing, 50*, 1530–1543.

Jackson, T.J., Cosh, M.H., Bindlish, R., Starks, P.J., Bosch, D.D., Seyfried, M., et al. (2010). Validation of advanced microwave scanning radiometer soil moisture products. *IEEE Transactions on Geoscience and Remote Sensing*, *48*(12), 4256–4272. http://dx.doi.org/10.1109/TGRS.2010.2051035.

Kerr, Y., Waldteufel, P., Richaume, P., Davenport, I., Ferrazzoli, P., & Wigneron, J. -P. (2008). *SMOS Level 2 Processor Soil Moisture ATBD.* Toulouse, France: CESBIO.

Kerr, Y.H., Waldteufel, P., Richaume, P., Wigneron, J.P., Ferrazzoli, P., Mahmoodi, A., et al. (2012). The SMOS soil moisture retrieval algorithm. *IEEE Transactions on Geoscience and Remote Sensing, 50*, 1384–1403.

Kerr, Y.H., Waldteufel, P., Wigneron, J.P., Delwart, S., Cabot, F., Boutin, J., et al. (2010). The SMOS mission: New tool for monitoring key elements of the global water cycle. *Proceedings of the IEEE, 98*, 666–687.

Kerr, Y.H., Waldteufel, P., Wigneron, J. -P., Martinuzzi, J., Font, J., & Berger, M. (2001). Soil moisture retrieval from space: The Soil Moisture and Ocean Salinity (SMOS) mission. *IEEE Transactions on Geoscience and Remote Sensing, 39*, 1729–1735.

Lau, W.K.M., & Kim, K. -M. (2012). The 2010 Pakistan flood and Russian heat wave: Teleconnection of hydrometeorological extremes. *Journal of Hydrometeorology, 13*(392–403), 2012.

Liu, Q., Reichle, R.H., Bindlish, R., Cosh, M.H., Crow, W.T., de Jeu, R.A.M., et al. (2011). The contributions of precipitation and soil moisture observations to the skill of soil moisture estimates in a land data assimilation system. *Journal of Hydrometeorology*, *12*, 750–765. http://dx.doi.org/10.1175/JHM-D-10-05000.1.

Loew, A., & Mauser, W. (2008). On the disaggregation of passive microwave soil moisture data using a priori knowledge of temporally persistent soil moisture fields. *IEEE Transactions on Geoscience and Remote Sensing*, *46*, 819–834. http://dx.doi.org/10.1109/TGRS.2007.914800.

Mahfouf, J., Brasnett, B., & Gagnon, S. (2007). A Canadian precipitation analysis (CaPA) project: Description and preliminary results. *Atmosphere-Ocean*, *45*, 1–17.

Mailhot, J., Bélair, S., Lefaivre, L., Bilodeau, B., Desgagné, M., Girard, et al. (2006). The 15-km version of the Canadian regional forecast, system. *Atmosphere-Ocean*, *44*, 133–149.

Martinez-Fernandez, J., & Ceballos, A. (2005). Mean soil moisture estimation using temporal stability analysis. *Journal of Hydrology*, *312*, 28–38. http://dx.doi.org/10.1016/j.jhydrol.2005.02.007.

Meng, X., Rosenthal, R., & Rubin, D.B. (1992). Comparing correlated correlation coefficients. *Psychological Bulletin*, *111*, 172–175.

Pietroniro, A., Fortin, V., Kouwen, N., Neal, C., Turcotte, R., Davison, B., et al. (2007). Development of the MESH modelling system for hydrological ensemble forecasting of the Laurentian Great Lakes at the regional scale. *Hydrology and Earth System Sciences*, *11*, 1279–1294.

Reichle, R.H. (2008). Data assimilation methods in the Earth sciences. *Advances in Water Resources*, *31*, 1411–1418.

Reichle, R.H., Crow, W.T., Koster, R.D., Sharif, H.O., & Mahanama, S.P.P. (2008a). Contribution of soil moisture retrievals to land data assimilation products. *Geophysical Research Letters*, *35*, L01404. http://dx.doi.org/10.1029/2007GL031986.

Reichle, R.H., Crow, W.T., & Keppenne, C.L. (2008b). An adaptive ensemble Kalman filter for soil moisture data assimilation. *Water Resources Research*, *44*, W03423. http://dx.doi.org/10.1029/2007WR006357.

Reichle, R.H., & Koster, R.D. (2004). Bias reduction in short records of satellite soil moisture. *Geophysical Research Letters*, *31*, L19501. http://dx.doi.org/10.1029/2004GL020938.

Reichle, R.H., & Koster, R.D. (2005). Global assimilation of satellite surface soil moisture retrievals into the NASA Catchment land surface model. *Geophysical Research Letters*, *32*, L02404. http://dx.doi.org/10.1029/2004GL021700.

Reichle, R., Koster, R., Liu, P., Mahanama, S., Njoku, E., & Owe, M. (2007). Comparison and assimilation of global soil moisture retrievals from the Advanced Microwave Scanning Radiometer for the Earth Observing System (AMSR-E) and the Scanning Multichannel Microwave Radiometer (SMMR). *Journal of Geophysical Research*, *112*, D09108. http://dx.doi.org/10.1029/2006JD008033.

Reichle, R.H., Walker, J.P., Koster, R.D., & Houser, P.R. (2002). Extended versus ensemble Kalman filtering for land data assimilation. *Journal of Hydrometeorology, 3*, 728–740.

Ridler, M. -E., Madsen, H., Stisen, S., Bircher, S., & Fensholt, R. (2014). Assimilation of SMOS-derived soil moisture in a fully integrated hydrological and soil-vegetation atmosphere transfer model in Western Denmark. *Water Resources Research*, *50*, 8962–8981. http://dx.doi.org/10.1002/2014WR015392.

Soulis, E.D., Snelgrove, K., Kouwen, N., Seglenieks, F., & Verseghy, D.L. (2000). Towards closing the vertical water balance in Canadian atmospheric models: Coupling of the land surface scheme CLASS with the distributed hydrological model WATFLOOD. *Atmosphere-Ocean*, *30*, 251–269.

Wolfson, N., Atlas, R., & Sud, Y.C. (1987). Numerical experiments related to the summer 1980 US heat wave. *Monthly Weather Review*, *115*, 1345–1357.

Xu, X., Li, J., & Tolson, B.A. (2014). Progress in integrating remote sensing data and hydrologic modeling. *Progress in Physical Geography*, *38*, 464–498. http://dx.doi.org/10.1177/0309133314536583.

Zeng, X., Wang, B., Zhang, Y., Song, S., Huang, X., Zheng, Y., et al. (2014). Sensitivity of high-temperature weather to initial soil moisture: A case study using the WRF model. *Atmospheric Chemistry and Physics*, *14*, 9623–9639.

Zhang, H., & Frederiksen, C.S. (2003). Local and nonlocal impacts of soil moisture initialization on AGCM seasonal forecasts: A model sensitivity study. *Journal of Climate*, *16*, 2117–2137.

Zhao, L., Yang, K., Qin, J., Chen, Y., Tang, W., Lu, H., et al. (2014). The scale-dependence of SMOS soil moisture accuracy and its improvement through land data assimilation in the central Tibetan Plateau. *Remote Sensing of Environment*, *152*, 345–355.